Polymer 50 (2009) 670–678

Contents lists available at ScienceDirect

Polymer

journal homepage: www.elsevier.com/locate/polymer

Effect of hydrophobic polystyrene microphases on temperature-responsive behavior of poly(*N*-isopropylacrylamide) hydrogels

Fangping Yi, Sixun Zheng*

Department of Polymer Science and Engineering, State Key Laboratory of Metal Matrix Composites, Shanghai Jiao Tong University, 800 Dongchuan Road, Shanghai 200240, China

ARTICLE INFO

Article history:
Received 8 June 2008
Received in revised form
17 November 2008
Accepted 21 November 2008
Available online 30 November 2008

Keywords:
Poly(*N*-isopropylacrylamide)
Hydrogels
Hydrophobic nanodomains

ABSTRACT

Reversible addition–fragmentation chain transfer polymerization was employed to prepare the crosslinked poly(*N*-isopropylacrylamide)-*graft*-polystyrene networks (PNIPAAm-*g*-PS). Due to the immiscibility of PNIPAAm with PS, the crosslinked PNIPAAm-*g*-PS copolymers displayed the microphase-separated morphology. While the PNIPAAm-*g*-PS copolymer networks were subjected to the swelling experiments, it is found that the PS block-containing PNIPAAm hydrogels significantly exhibited faster response to the external temperature changes according to swelling, deswelling, and reswelling experiments than the conventional PNIPAAm hydrogels. The improved thermo-responsive properties of hydrogels have been interpreted on the basis of the formation of the specific microphase-separated morphology in the hydrogels, *i.e.*, the PS blocks pendent from the crosslinked PNIPAAm networks were self-assembled into the highly hydrophobic nanodomains, which behave as the microporogens and thus promote the contact of PNIPAAm chains and water. The self-organized morphology in the hydrogels was further confirmed by photon correlation spectroscopy (PCS). The PCS shows that the linear model block copolymers of PNIPAAm-*g*-PS networks were self-organized into micelle structures, *i.e.*, the PS domains constitute the hydrophobic nanodomains in PNIPAAm-*g*-PS networks.

1. Introduction

Hydrogels are a class of crosslinked polymers that are swollen in water without dissolving. Owing to their biocompatibility, special surface properties and high water content, hydrogels have been the materials of choice in many biomedical applications [1–4]. The hydrogels based on poly(*N*-alkylacrylamide)s such as poly(*N*-isopropylacrylamide) and poly(*N*,*N*′-dimethylacrylamide) are among the most-investigated systems since they possess some attractive environment-responsive properties [5–13]. For instance, poly(*N*-isopropylacrylamide) (PNIPAAm) hydrogels can exhibit typical volume-phase transition temperature (VPTT) behavior [5–7,14]. The volume-phase transfer properties stem from the behavior of lower critical solution temperature (LCST) around ~32 °C of PNIPAAm in aqueous solution [15–20]. At lower temperatures individual PNIAPM chains in aqueous solution extend with a random coil conformation but collapse into a globule while the solution temperature is higher than 32 °C. In addition, these polymeric hydrogels can also display clear volume-phase transition in response to other external stimuli such as pH [14,21,22], composition of solvents [5,6,23–26], salt concentration [6,10], light [7,27], mechanical stress [28,29], and magnetic field [30,31]. The environment-sensitive properties endow these polymer systems with a promising potential for application in biomedical areas.

Poly(*N*-alkylacrylamide) hydrogels can be prepared through conventional radical copolymerization of *N*-alkylacrylamides with bifunctional organic crosslinking agent such as *N*,*N*′-methylenebisacrylamide. However, these conventional hydrogels inherently possess some drawbacks in morphology and properties such as morphological inhomogeneity, low mechanical strength and slow swelling and deswelling rates. It has been proposed that these disadvantages are responsible for the inherent problems of chemically crosslinked polymer networks, *i.e.*, broad distribution of polymer chain lengths between crosslinking points [29,32–35]. During the past years, considerable effort has been done to improve the properties of hydrogels. For instance, faster swelling and deswelling can be achieved by introducing porosities and structural inhomogeneity [36–43]. However, care must be taken as the mechanical properties of porous hydrogels can be significantly lower than nonporous hydrogels. Therefore, the measures for improving this property of porous hydrogels must be taken to balance with ratio of swelling and fast response rates. Recently, it is reported that the enhancement of temperature-response rate of hydrogels can be achieved through introduction of structural inhomogeneity into the systems [44–46]. The structural inhomogeneity can be either hydrophilic or hydrophobic [34,47–52].

* Corresponding author. Tel.: +86 21 54743278; fax: +86 21 54741297.
E-mail address: szheng@sjtu.edu.cn (S. Zheng).

0032-3861/$ – see front matter © 2008 Elsevier Ltd. All rights reserved.
doi:10.1016/j.polymer.2008.11.038

Yoshida et al. [34] found that grafting freely mobile, pendent poly(ethylene oxide) (PEO) chains, a water-soluble block, into PNIPAAm networks could dramatically enhance the shrinking rate of the hydrogels. Lee et al. [47] introduced the hydrophilic alginate (or sodium alginate) into PNIAPAM and found that the comb-shaped composite hydrogels were able to respond rapidly to both temperature and pH changes. It has been reported that the unique architecture of grafted hydrogels can find a number of applications in the area of biotechnology such as drug delivery systems [48], size-selective bio-separation [49,50] and enzyme and cell immobilizations [51]. It is proposed that in the water-swollen systems, these hydrophilic modifiers will not demix to form separated domains, *i.e.*, the hydrogels remain homogeneous. More recently, it is identified that the incorporation of hydrophobic blocks (or segments) into PNIPAAm hydrogels can alternatively improve the properties of hydrogels [32,53–59]. For instance, Zhang and Zhuo [53] reported the modification of PNIPAAm hydrogels by introducing hydrophobic inorganic segments. They prepared the organic–inorganic hybrid hydrogels by copolymerizing NIPAAm with vinyltriethoxysilane and thus the polysilsesquioxane linkages were incorporated into the hydrogels; they found that the response rates of the hydrogels were significantly improved. Haraguchi et al. [32,35,54] prepared an organic–inorganic nanocomposite PNIPAAm hydrogel, in which exfoliated clay layers acted as effective multifunctional crosslinking agents and the hydrogel properties were significantly improved. In a previous work, we reported the modification *via in situ* crosslinking of PNIPAAm using a hydrophobic polyhedral oligomeric silsesquioxane (POSS) macromer. It is noted that the temperature response of the POSS-crosslinked PNPAM hydrogels was significantly improved compared to the control hydrogels [56].

Although the inclusion of hydrophobic blocks can alternatively improve the properties of hydrogels, this approach could follow the mechanisms different from the improvement of hydrogel properties *via* incorporation of hydrophilic components. It is plausible to propose that the hydrophobic components in hydrogels could behave as microporogens and thus the area of the contact interfaces between PNIPAAm chain and water molecules are significantly increased. The increased area of contact interfaces between PNIPAAm chain and water molecules could facilitate the diffusion of water molecules in the crosslinked networks, *i.e.*, the hydrophobic microdomains could also act as tunnels in which water molecules go through and thus accelerate the diffusion of water molecules. In addition, the aggregated hydrophobic microdomains could act as the physical crosslinking sites of the hydrogels and thus the overall crosslinking density of hydrogels was increased. Nonetheless, such a investigation remains largely unexplored vis-à-vis modification of hydrogels with hydrophilic components.

In the present work, we present an investigation on a model PNIPAAm network, in which the hydrophobic polystyrene (PS) chains were grafted on PNIPAAm networks as pendent chains. Toward this end, a reversible addition–fragmentation transfer (RAFT) polymerization is employed. In the first step, the PS macromolecular chain transfer agent (PS-CTA) with defined length was prepared and then the RAFT polymerizations among NIPAM, PS-CTA and *N*,*N*-methylenebisacrylamide (BIS) were carried out to afford the PNIPAAm-*g*-PS networks. The behavior of hydrogels was addressed on the basis of swelling, deswelling and reswelling kinetics.

2. Experimental

2.1. Materials

2,2-Azobisisobutylnitrile (AIBN) and *N*,*N*′-methylenebisacrylamide (BIS) were of chemically pure grade, supplied by Shanghai Reagent Co., Shanghai, China. *N*-Isopropylacrylamide (NIPAM) was prepared in this laboratory by following the literature method [60]. Styrene is of analytically pure grade, purchased from Shanghai Reagent Co., China. Prior to use, the inhibitor was removed by washing with aqueous sodium hydroxide (5 wt%) and deionized water, respectively, for at least three times; the monomer was dried by anhydrous $MgSO_4$ and then distilled at reduced pressure. The solvent, tetrahydrofuran (THF) was dried by reflux over sodium and then distilled. All other reagents were purified by common purification procedures.

2.1.1. Synthesis of PS macromolecular chain transfer agent (PS-CTA)

2-Phenylpropyldithiobenzoate was prepared by following the literature method [61]. In the first step, dithiobenzoic acid was prepared *via* the reaction between Grignard reagent and carbon disulfide [61]. The Grignard reagent was prepared from bromobenzene (5.60 g, 0.036 mol) and magnesium (0.820 g, 0.0360 mol) and iodine (35 mg, 0.28 mmol) in anhydrous tetrahydrofuran (100 ml) and the solution was heated up to 45 °C with stirring. Carbon disulfide (2.70 g, 0.036 mol, dissolved in 30 ml tetrahydrofuran) was dropped into the solution of Grignard reagent at −5 °C within 30 min. The system was maintained at this temperature for additional 1 h with vigorous stirring and 50 ml 5% cold aqueous hydrochloric acid was added with stirring. The organic layer was separated with diethyl ether and then extracted with 10% cold aqueous sodium hydroxide (30 ml × 3). The alkaline solution was washed with diethyl ether three times and acidified with 10% cold aqueous hydrochloric acid and finally extracted with diethyl ether. The ether layer was washed with deionized water three times to neutrality. The solvent was removed *via* rotary evaporation and the product (*viz.* dithiobenzoic acid) was obtained with the yield of 70%. Dithiobenzoic acid was used to prepare 2-phenylpropyldithiobenzoate. To a flask dithiobenzoic acid (10.59 g, 0.0688 mol), α-methylstyrene (10.0 g, 0.0847 mol) and carbon tetrachloride (40 ml) were charged. The reaction was carried out at 70 °C for 6 h with vigorous stirring. The crude product was purified by column chromatography on alumina oxide with *n*-hexane as the eluent to afford 2-phenylpropyldithiobenzoate as dark purple oil with the yield of 28.6%. ^{1}H NMR ($CDCl_3$, ppm): 2.01 [*s*, 6**H**, –C(C**H**$_3$)$_2$–]; 7.16–7.85 (m, 10**H**, proton of aromatic ring).

2-Phenylpropyldithiobenzoate was used as a chain transfer agent of RAFT polymerization to prepare polystyrene macromolecular chain transfer agent (PS-CTA). Typically, styrene (9.00 g, 86.5 mmol), 2-phenylpropyldithiobenzoate (24.6 mg, 0.90 mmol) and AIBN (48.0 mg, 0.30 mmol) were added to a 25 ml flask equipped with magnetic stirrer. The system was connected to a standard Schlenk line to degas by three freeze–evacuate–thaw cycles. The flask was sealed under high vacuum and then placed in an oil bath at 110 °C; the polymerization was carried out for 15 h. The crude product was dropped into an excess methanol to afford the precipitates. The precipitates were dissolved with THF and re-precipitated using methanol. This procedure was repeated for three times to purify the macromolecular chain transfer agent, which was dried in a vacuum oven at 30 °C for 24 h. The product (4.60 g) was obtained with the yield of 50.3%. The molecular weight was estimated according to the ratio of integration intensity of aromatic protons of 2-phenylpropyldithiobenzoate moiety to that of aromatic proton of styrene moiety in ^{1}H NMR spectrum and calculated to be $M = 6100$ [61].

2.1.2. Preparation of PNIPAAm-g-PS networks

The PNIPA-*g*-PS networks were prepared *via* RAFT polymerization in the presence of PS macromolecular chain transfer agent (PS-CTA) with the content of PS block up to 20 wt%. Typically, to a glass tube equipped with a dry magnetic stirrer, NIPAAm (2.25 g, 19.9 mmol), PS-CTA (0.200 g, 0.0326 mmol) and BIS (0.0307 g,

0.199 mmol) and 2 ml anhydrous THF were charged and AIBN (0.0018 g, 0.0109 mmol) was added as the initiator. The system was connected to a standard Schlenk line, degassed using three freeze–evacuate–thaw cycles and then sealed. The glass tube was immersed in a thermostated oil bath and the polymerization was carried out at 90 °C for 30 h. In order to remove any unreacted NIPAAm monomer the crosslinking product was dialyzed with deionized water for four days. After drying *in vacuo* at 30 °C for 24 h, the crosslinked product was weighed and the conversion of the monomer was calculated to be about 90%.

2.1.3. Synthesis of model PNIPAAm-b-PS block copolymers

The synthetic procedure of the model PNIPAAm-*b*-PS block copolymers is similar to that of PNIPAAm-*g*-PS networks. In a typical experiment, to a 25 ml glass tube, PS-CTA (1.00 g, 0.163 mmol), NIPAAm (4.25 g, 37.6 mmol), AIBN (0.0063 g, 0.0380 mmol) and THF (4 ml) were charged. The mixture was degassed *via* three freeze–evacuate–thaw cycles and the tube was sealed under high vacuum. The polymerization was carried out at 90 °C for 30 h. The crude polymer was dissolved in THF and the mixture was precipitated in excess petroleum ether. This procedure was repeated for three times to purify the products. After drying in a vacuum oven at 30 °C, 3.98 g polymer was obtained with the conversion of NIPAAm monomer to be 70%. The GPC was used to measure the molecular weights of the model diblock copolymers, relative to polystyrene standard. The results of molecular weights are summarized in Table 1.

2.1.4. Measurement and techniques

2.1.4.1. Nuclear magnetic resonance spectroscopy (NMR). The ^{1}H NMR spectra were recorded on a Varian Mercury Plus 400 MHz NMR spectrometer at room temperature. The samples were dissolved with the deuterated chloroform, and the solutions were measured with tetramethylsilane (TMS) as an internal reference.

2.1.4.2. Fourier transform infrared spectroscopy (FTIR). The FTIR measurements were conducted on a Perkin–Elmer Paragon 1000 Fourier transform spectrometer at room temperature (25 °C). The sample films were prepared by dissolving the polymers with THF (5 wt%) and the solutions were cast onto KBr windows. The residual solvent was removed in a vacuum oven at 60 °C for 2 h. The crosslinked samples were granulated, and the powder was mixed with KBr pellets to press into small flakes for measurements. All of the specimens were sufficiently thin to be within a range where the Beer–Lambert law is obeyed. In all cases, 64 scans at a resolution of 2 cm^{-1} were used to record the spectra.

2.1.4.3. Gel permeation chromatography. The molecular weights of the model PNIPAAm-*b*-PS dibock copolymers were measured by gel permeation chromatography (GPC) at 70 °C on a Perkin–Elmer Series 200 system (100 μL injection column, 10 μm PL gel 300 mm × 7.5 mm mixed B columns) equipped with a RI detector. *N*,*N*′-dimethylformamide (DMF) containing 0.01 mol/L lithium bromide was used as a eluent at a flow rate of 1.0 ml/min. The column system was calibrated by standard polystyrene.

Table 1
Results of polymerization for the preparation of PNIPAAm-*g*-PS networks and PNIPAAm-*b*-S diblock copolymers.

Samples	Feed of PS (wt%)	Conversion of NIPAAm (mol%)	PS Content (wt%)	M_n	M_w/M_n
PNIPAAm-*g*-PS5	5.0	94.5	5.3	–	–
PNIPAAm-*g*-PS7.5	7.5	95.6	7.8	–	–
PNIPAAm-*g*-PS10	10.0	90.0	10.9	–	–
PNIPAAm-*g*-PS15	15.0	94.9	15.7	–	–
PNIPAAm-*g*-PS20	20.0	92.8	21.2	–	–
PNIPAAm-*b*-PS5	5.0	78.3	6.3	92,300	1.60
PNIPAAm-*b*-PS20	20.0	91.3	21.5	28,600	1.26

2.1.4.4. Differential scanning calorimetry (DSC). Differential scanning calorimetry (DSC) was carried out with a Perkin–Elmer Pyris 1 differential scanning calorimeter in a dry nitrogen atmosphere. An indium standard was used for temperature and enthalpy calibrations, respectively. All of the samples (about 15.0 mg in weight) were first heated to 160 °C and held at this temperature for 3 min to remove the thermal history, followed by quenching to 0 °C. A heating rate of 20 °C/min was used at all cases. Glass transition temperatures (T_g) were taken as the midpoint of the heat capacity change.

2.1.4.5. Atomic force microscopy (AFM). The samples for AFM measurement were prepared *via* spin coating the solution of the block copolymers on cleaned glass sliders. The block copolymers were dissolved in methanol to prepare the solution with the concentration of 20 wt%; the solution was spin-coated at the speed of 1000 rpm on cleaned glass slides to form a flat and thin layer. The specimens were further dried *in vacuo* at 150 °C for 30 min and the thickness of films was estimated to be 20 μm. The AFM experiments were performed with a Nanoscope IIIa scanning probe microscope (Digital Instruments, Santa Barbara, CA). Contacting mode was employed in air using a tip fabricated from silicon (125 μm in length with *ca.* 500 kHz resonant frequency). Typical scan speeds during recording were 0.3–1 lines × s^{-1} using scan heads with a maximum range of 5 μm × 5 μm.

2.1.4.6. Photon correlation spectroscopy (PCS). The linear block copolymers (0.01 g) were dissolved in 0.5 ml THF and then 50 ml ultra-pure water was added dropwise by a dropping funnel with vigorous stirring. After additional stirring for 30 min, a transparent emulsion was formed with the concentration of the copolymer being 0.02 wt%. The PCS measurement was carried out on a Zetasizer 3000HSA (Malvem Instrument, Malvem, Worcestershire, UK) with a He–Ne laser operating at the wavelength of 633 nm. The scattering angle for size analysis was fixed at 90°. All measurements were carried out at 20 °C and solvent refractive index was set to 1.330 and solvent viscosity to 1.00 for analysis.

2.1.4.7. Swelling, deswelling and reswelling kinetics of hydrogels. The specimens for swelling, deswelling and reswelling experiments were cut from the dried cylindered samples with the identical diameter and the heights of specimens were controlled to be *ca.* 5 mm. Swelling ratios of the hydrogels were gravimetrically measured after wiping off the water on the surface with moistened filter paper in the temperature range from 22 to 48 °C. All of the gel samples were dipped in distilled water for at least 24 h at every particular temperature. Swelling ratio (SR) is defined as follows:

$$SR = W_s/W_d \quad (1)$$

where W_s is the weight of the water in the swollen gel at a particular temperature and W_d is the dry weight of the gel.

The deswelling kinetics of hydrogels was gravimetrically measured at 48 °C after wiping off water on the surface with moistened filter paper. Prior to the measurement, the gel samples were equilibrated in distilled water at room temperature (25 °C) for 24 h. The weight changes of gels were recorded with regular time intervals. Water retention (WR) is defined as follows:

$$WR = (W_t - W_d)/W_s \times 100\% \quad (2)$$

where W_t is the weight of the gel at regular time intervals and the other symbols are the same as defined above.

The kinetics of reswelling of hydrogels was gravimetrically measured at 22 °C. Since the utilization of gel devices in practical

applications is impossibly in a dried state before reabsorbing water, the reswelling kinetics of gels was measured at the equilibrium in distilled water at 48 °C for 24 h. After wiping off water on the surface, the weight changes of gels were recorded at regular time intervals. Water uptake (WU) is defined as follows:

$$\mathrm{WU} = (W_t - W_d)/W_s \times 100\% \quad (3)$$

where W_t is the weight of the gels at regular time intervals and the other symbols are the same as defined above.

3. Results and discussion

3.1. Synthesis and characterization of PNIPAAm-g-PS networks

Reversible addition–fragmentation chain transfer (RAFT) polymerization is a versatile and controllable radical polymerization technique for the synthesis of a variety of polymers with well-defined topological structures and architectures [59]. In this work, the RAFT polymerization was explored to access the poly(*N*-isopropylacrylamide)-*graft*-polystyrene copolymer networks. The synthesis route of the networks is shown in Scheme 1. In the first step, the polystyrene macromolecular chain transfer agent (PS-CTA) was prepared with the RAFT polymerization of styrene with 2-phenylpropyldithiobenzoate as the chain transfer agent and with 2,2-azobisisobutylnitrile (AIBN) as the initiator. 2-Phenylpropyldithiobenzoate was prepared *via* the addition reaction of dithiobenzoic with α-methylstyrene by following the literature method [61]. PS-CTA with the desired chain length was obtained by controlling the conversion of styrene in the polymerization. In this case, the molecular weight of PS-CTA was controlled to be $M_n = 6100$, which was estimated according to the ratio of integration intensity of 2-phenylpropyldithiobenzoate to styrene moiety protons in the ^{1}H NMR spectrum of PS-CTA shown in Fig. 1. The PS-CTA with the defined length was used as the macromolecular RAFT chain transfer agent to prepare the poly(*N*-isopropylacrylamide)-*graft*-polystyrene copolymer networks (PNIPAAm-*g*-PS) with *N*,*N*-methylenebisacrylamide (BIS) and AIBN as the crosslinking agent and initiator, respectively. It is proposed that with the RAFT polymerization of NIPAAm and BIS the PS existed in the PNIPAAm-*g*-PS crosslinked networks in the form of pendent side chains due to the reversible addition–fragmentation chain transfer reaction. With the polymerization proceeding, the systems were gradually gelled, suggesting the formation of crosslinked networks. To verify the occurrence of the crosslinking reaction involved with PS-CTA, the linear model PNIPAAm-*b*-PS diblock copolymers were also synthesized under the identical conditions. The difference in polymerization between the PNIPAAm-*g*-PS networks and PNIPAAm-*b*-PS diblock copolymers rests with the utilization of BIS, a bifunctional crosslinking agent. The ^{1}H NMR spectrum as well as the assignment of the spectrum of PNIPAAm-*b*-PS diblock copolymer is incorporated into Fig. 1 (Curve A). The resonance in the range of 6.0–7.5 ppm was ascribed to the aromatic proton of styrene chains whereas the resonances at 3.98 and 1.13 ppm were assignable to the protons of amide and methyl groups in isopropylacrylamide structural units. The PNIPAAm-*g*-PS networks were dialyzed with deionized water to remove the unreacted NIPAAm and the real compositions of the crosslinked PNIPAAm-*g*-PS copolymer networks are calculated as summarized in Table 1. It is noted out that within the sufficient time of reaction the conversion of PNIPAAm can attain more than 90 wt%. Representatively shown in Fig. 2 are Fourier transform infrared spectroscopy (FTIR) of the control PNIPAAm and PNIPAAm-*g*-PS network containing 5 wt% PS. The control PNIPAAm is characterized by N–H stretching vibration bands in the range of 3200–3600 cm^{-1} as well as amide I band at ~1649 cm^{-1} and amide II band at ~1546 cm^{-1}.

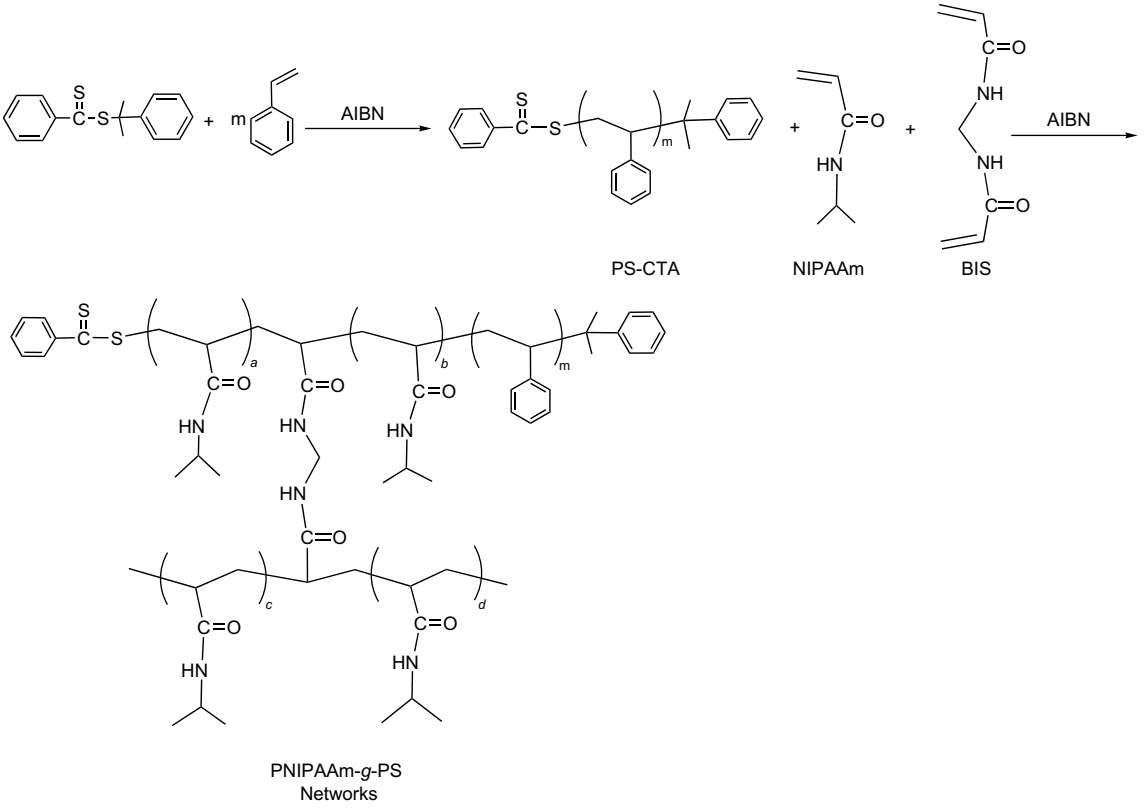

Scheme 1. Synthesis of PS-CTA and PNIPAAm-*g*-PS copolymer networks.

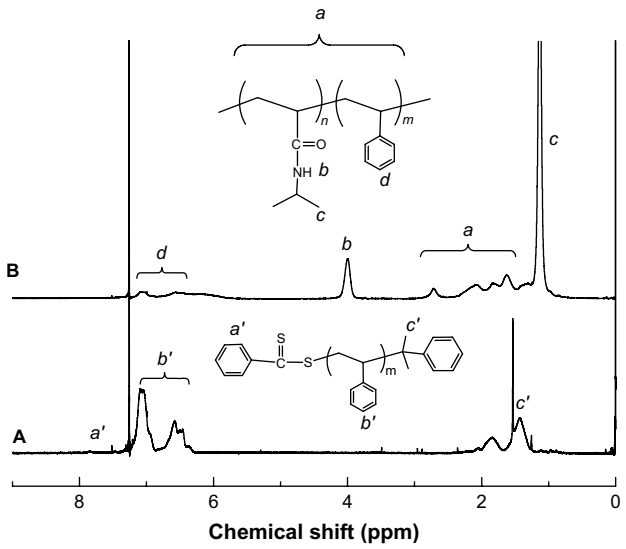

Fig. 1. ^{1}H NMR spectra of PS-CTA (A) and PNIPAAm-*b*-PS5 (B).

For the PNIPAAm-*g*-PS10 network, the in-plane bending vibration of C–H bonds for mono-substituted aromatic ring occurred at 700 and 750 cm^{-1}. The band at 3027 cm^{-1} is assigned to the stretching vibration of C–H bonds of aromatic ring of PS chains, which indicates the presence of PS structure. The FTIR spectroscopy shows that the resulting networks combined the structural features from PNIPAAm and PS. It is proposed that with the designed approach of polymerization, the PS component exits in the crosslinked network as pendent side chains. In order to investigate the morphology of the PNIPAAm-*g*-PS copolymer networks, all the crosslinked products were subjected to differential scanning calorimetry (DSC). The DSC curves are shown in Fig. 3. The control PNIPAAm displayed a glass transition at 141 °C and the PS-CTA exhibited the lower glass transition at 78 °C. The fact that the T_g of the PS-CTA is much lower than that of PS thermoplastic (*e.g.*, 100 °C) is responsible for its relatively low molecular weight. All the crosslinked PNIPAAm-*g*-PS copolymer networks displayed the discernible glass transition at the constant temperature (~141 °C), which are assignable to PNIPAAm matrix. It is noted that the T_gs of PNIPAAm matrix remain invariant irrespective of the inclusion of PS pendent side chains

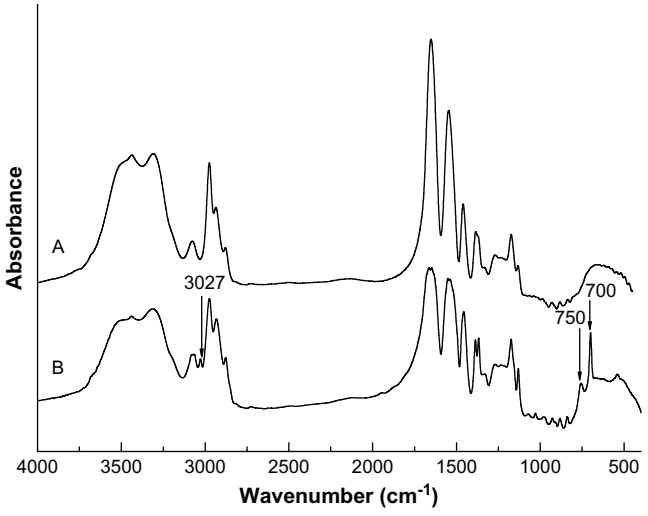

Fig. 2. FTIR spectra of the control PNIPAAm (A) and PNIPAAm-*g*-PS network containing 5 wt% PS (B).

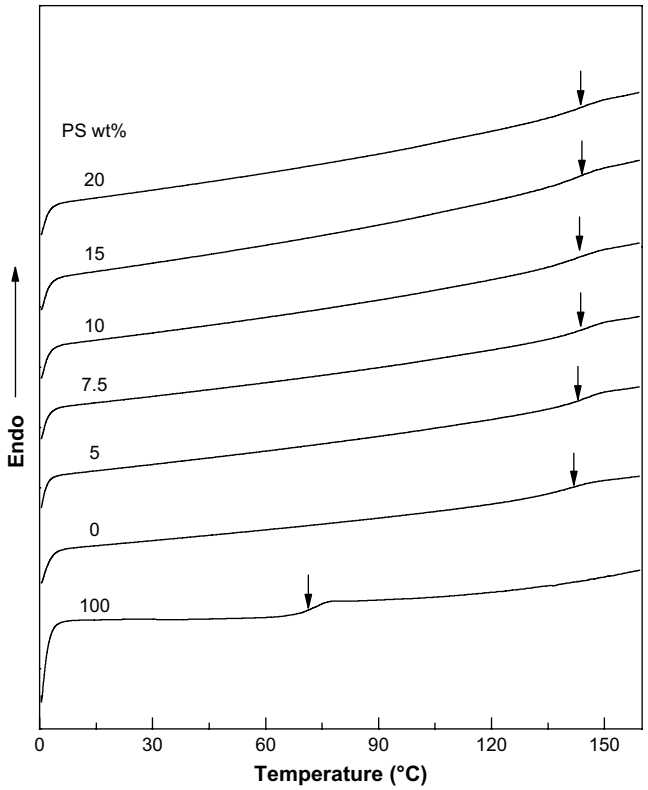

Fig. 3. DSC curves of PS-CTA, the control PNIPAAm network and the PNIPAAm-*g*-PS networks.

although the T_gs of the PS are much lower than that of PNIPAAm. This observation suggests that the glass transition of the PNIPAAm matrix is less affected by the PS side chains. In other words, the PNIPAAm matrix is immiscible with the PS side chain, *i.e.*, the PNIPAAm-*g*-PS copolymer networks are microphase separated and existed in the form of dispersed nanodomains in the continuous PNIPAAm matrix [62,63].

The formation of the microphase-separated morphology (or nanostructures) in the PNIPAAm-*g*-PS copolymer networks can be further evidenced by atomic force microscopy (AFM). Toward this end, the model PNIPAAm-*b*-PS diblock copolymers with the identical composition with the PNIPAAm-*g*-PS copolymer networks were synthesized *via* the sequential RAFT polymerization. The specimens were prepared *via* spin coating of the THF solution of the diblock copolymers onto glass slides and the films were subjected to morphological observation by means of AFM. Representatively shown in Fig. 4 are the micrographs of AFM in contact mode for the copolymer containing 10 wt% PS. It is seen that the microphase-separated morphology was obtained. In terms of the volume fraction of PS and the difference in viscoelastic properties between PNIPAAm and PS domains, the light continuous regions could be ascribed to the PNIPAAm matrix whilst the spherical dark regions are assignable to PS domains. It is seen that the PS microphase at the size of 10–30 nm (in diameter) was dispersed in the continuous PNIPAAm. The AFM suggests that the PNIPAAm-*g*-PS copolymer networks could be microphase separated, *i.e.*, the crosslinked networks displayed the nanostructures. It is proposed that the PS nanodomains will be reserved whereas PNIPAAm matrix is significantly swollen while the PNIPAAm-*g*-PS copolymer networks are subjected to swelling experiments because PS is insoluble in water. The inhomogeneous morphology at the nanoscaled scale could exert a profound impact on the properties of the PNIPAAm-*g*-PS hydrogels.

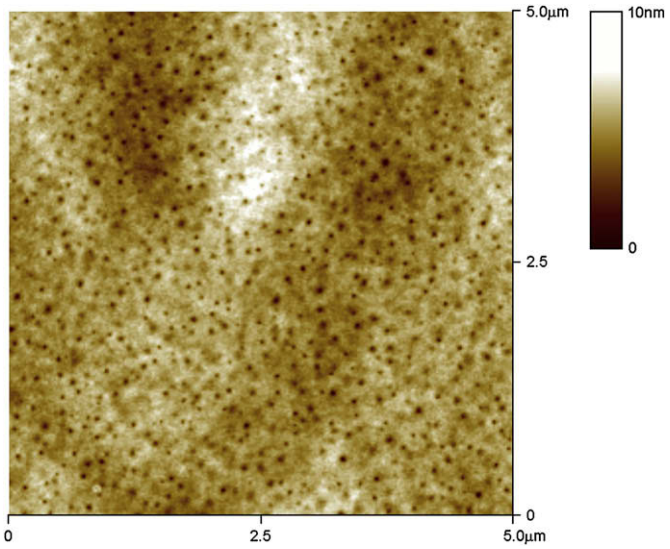

Fig. 4. AFM images of PNIPAAm-*b*-PS block copolymer containing 10 wt% of PS.

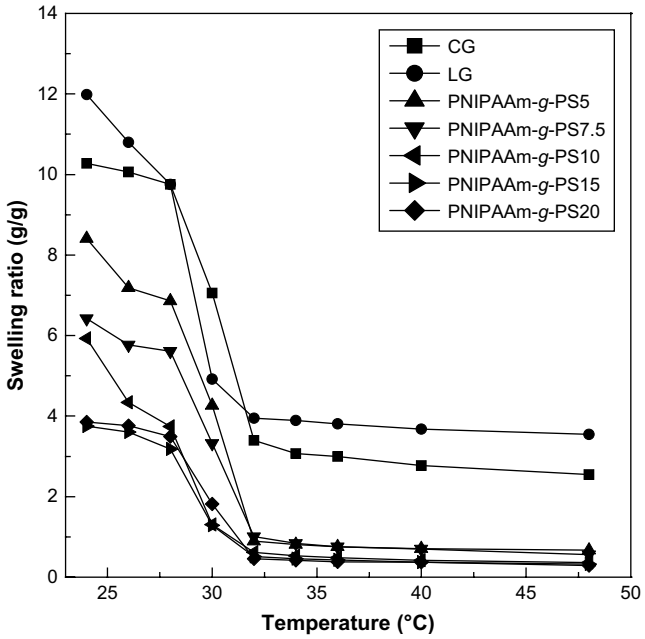

Fig. 5. Plots of equilibrium swelling ratio as functions of temperature for the control and PNIPAAm-*g*-PS hydrogels. CG: hydrogel prepared *via* conventional radical polymerization; LG: hydrogel prepared *via* RAFT polymerization.

3.2. Swelling kinetics of PNIPAAm-g-PS hydrogels

The PNIPAAm-*g*-PS networks were subjected to the swelling experiments in water. All the polymer networks can be swollen without dissolving, suggesting the formation of crosslinked structures. It is seen that at low temperature (*e.g.*,<30 °C) the PNIPAAm-*g*-PS hydrogels were homogeneous and translucent. When heated up to the higher temperatures (*e.g.*, >40 °C), the hydrogels became shrank and cloudy, implying the occurrence of volume-phase transition (VPT) phenomenon. Re-cooled to the low temperatures, the hydrogels can be re-swollen and became translucent again. This observation indicates that all the PNIPAAm-*g*-PS hydrogels possess temperature-sensitive properties as the control PNIPAAm hydrogel. It is of interest to investigate the swelling, deswelling and reswelling kinetics of the PNIPAAm-*g*-PS hydrogels.

3.2.1. Swelling behavior

The above PNIPAAm-*g*-PS hydrogels were employed to investigate the swelling and deswelling kinetics. The plots of stable swelling ratios as a function of temperature are shown in Fig. 5. For comparison, the swelling behavior of the control PNIPAAm hydrogel prepared *via* the conventional radical polymerization between NIPAM and BIS (denoted CG) was also incorporated into Fig. 5. Each hydrogel diaplayed a sigmoid curve of swelling ratio *versus* temperature, which is characteristic of volume-phase transition behavior of temperature-responsive hydrogels. In views of swelling curves, it is seen that the PNIPAAm-*g*-PS hydrogels exhibited the clear volume-phase transition in the neighbour of 32 °C. Compared to the control hydrogels, the curves of swelling ratio *versus* temperature slightly shifted the lower temperatures with the inclusion of PS. Below the volume-phase transition temperatures (VPTTs) the PNIPAAm-*g*-PS hydrogels possessed lower swelling ratios than the control PNIPAAm hydrogels and the swelling ratios were decreased with increasing the content of PS. This observation is ascribed to the decrease in the relative portion of hydrophilic components (*i.e.*, PNIPAAm) due to the inclusion of the hydrophobic component (*viz.* PS). Nonetheless, it is noted that above the volume-phase transfer temperatures (VPTTs), all the PNIPAAm-*g*-PS hydrogels displayed the swelling ratios much lower than the control PNIPAAm hydrogels (*e.g.*, CG) at the identical temperatures. In other words, the PNIPAAm-*g*-PS hydrogels facilitate the release of water compared to the control hydrogels upon heating the hydrogels above the VPTT. In addition, it is of interest to note that under the identical condition the pure PNIPAAm hydrogel prepared from RAFT polymerization (LG) displayed higher swelling ratio than the PNIPAAm hydrogels prepared *via* conventional radical polymerization (CG) when the temperature is below the VPTT. When the temperature is above the VPTT, the LG also displayed much lower swelling ratio than CG. It has been known that the hydrogels prepared *via* conventional radical polymerization could inherently possess some drawbacks in morphology and properties such as morphological inhomogeneity, low mechanical strength and slow swelling and deswelling rates. It is proposed that these disadvantages could result from the uncontrolled radical polymerization, *i.e.*, the conventional radical polymerization results in the inherent problems of chemically crosslinked polymer networks, *i.e.*, broad distribution of polymer chain lengths between crosslinking points [29,32–35]. Haraguchi et al. [35,54] proposed that the structural drawbacks are one of the major causes for the poor properties of hydrogels. In the present case, the improved properties for the PNIPAAm hydrogels *via* the controlled polymerization could reflect the structural homogeneity of crosslinked networks superior to the conventional radical polymerization.

3.2.2. Deswelling behavior

The deswelling kinetics was evaluated by measuring the swelling ratios of the hydrogels at 48 °C for various times. The deswelling curves are shown in Fig. 6. All the hydrogels shrinked and lost the absorbed water while they were heated up to the temperatures above the VPTT. However, it is worth noticing that upon deswelling the PNIPAAm-*g*-PS hydrogels displayed much lower stable water retention within the identical time than the control PNIPAAm hydrogels. This observation suggests that the deswelling of the PNIPAAm-*g*-PS hydrogels attained to its stable water retention is much faster than the control PNIPAAm hydrogels. For example, it takes *ca.* 10 min to reach the stable water retention of *ca.* 30% (or 48%) for the LG (or CG). For the PNIPAAm-*g*-PS hydrogels, all the stable water retentions are lower than 20% within the identical time. For the PNIPAAm-*g*-PS7.5 hydrogel, the stable water retention is even as low as 10 %. This observation suggests that within the identical time, the PNIPAAm-*g*-PS

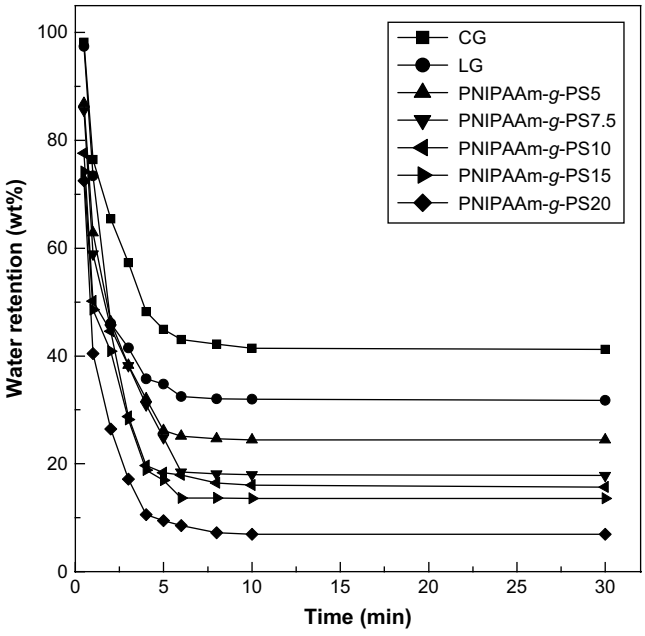

Fig. 6. Plots of water retention as functions of deswelling time at 48 °C for the measurement of deswelling kinetics of the hydrogels. CG: hydrogel prepared *via* conventional radical polymerization; LG: hydrogel prepared *via* RAFT polymerization.

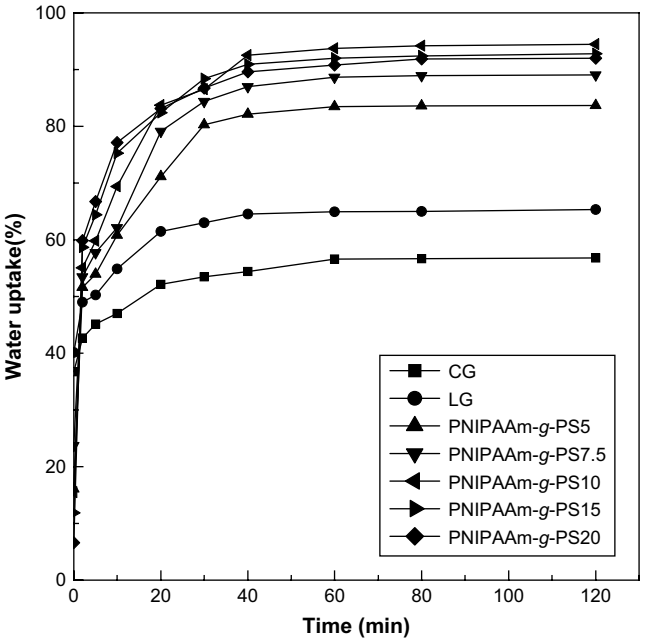

Fig. 7. Plots of water uptake as functions of reswelling time for the evaluation of reswelling kinetics of the hydrogels. CG: hydrogel prepared *via* conventional radical polymerization; LG: hydrogel prepared *via* RAFT polymerization.

hydrogels are capable of releasing much more absorbed water than the control hydrogels. In addition, it is of interest to note that the deswelling rate of LG is much faster than CG.

3.2.3. Reswelling behavior

Fig. 7 shows the plots of water uptake of the hydrogels as a function of time. In the experiments, all the hydrogels were firstly deswollen to reach the equilibria at 48 °C in the distilled water, and then the reswelling ratios of the hydrogels were measured gravimetrically at 22 °C, which are quite lower than the VPTTs of the hydrogels. It is seen that the PNIPAAm-*g*-PS hydrogels gave the higher water uptakes than the control hydrogels after the 10-min induction period elapsed. For the control PNIPAAm hydrogel *via* the conventional radical polymerization, it takes 60 min to attain the stable water uptake of 58 wt%. With the identical time, the stable water uptakes of the PNIPAAm-*g*-PS hydrogels are much higher than this value; the PNIPAAm-*g*-PS10 hydrogel gave the highest water uptake. This observation indicates that the reswelling of the PNIPAAm-*g*-PS hydrogels is much faster than the control PNIPAAm hydrogels. The increased rates of the PNIPAAm-*g*-PS hydrogels could be responsible for the formation of the specific nanostructures (See below). It is also of interest to note that with the identical time, the water uptakes of the control hydrogel prepared *via* RAFT polymerization are also significantly higher than that of the control hydrogel *via* the conventional radical polymerization.

3.3. Interpretation of PNIPAAm-g-PS hydrogel behavior

In this work, all the PNIPAAm networks were prepared *via* RAFT polymerization. In views of the comparison of control hydrogel behavior between CG and LG, the improved properties of hydrogels for the control LG could be attributed to the use of the approach of RAFT polymerization. The RAFT polymerization is carried out in a living and controlled fashion [59,61], which to some extent overcomes the limitations of the conventional radical polymerization for the preparation of hydrogels. The conventional PNIPAAm hydrogels inherently displayed morphological inhomogeneity, low mechanical strength, low swelling ratio at equilibrium and slow swelling and deswelling rates. It has been proposed that all these disadvantages are responsible for the broad distribution of polymer chain lengths between crosslinking points of the crosslinked networks which result from the uncontrolled radical polymerization [29,32–35]. For the modified hydrogels, it is seen that all the PNIPAAm-*g*-PS copolymer networks are homogenous and translucent, suggesting that no macroscopic phase separation occurred. In other words, the phase separation (if any) occurred at the scale smaller than the length of visible lights. The formation of microphase-separated morphology (or nanostructures) was further evidenced by atomic force microscopy (AFM) with the model PNIPAAm-*b*-PS diblock copolymers (See Fig. 4). It is plausible to propose that the PNIPAAm-*g*-PS networks displayed the microphase-separated morphology, in which the PS nanodomains were dispersed in the continuous PNIPAAm matrix. The formation of the nanostructures in the PNIPAAm-*g*-PS copolymer networks is ascribed to the immiscibility between PNIPAAm and PS (See Scheme 2). The PS nanodomains can be dissolved in organic solvent such as tetrahydrofuran. Nonetheless, the crosslinked PNIPAAm matrices could be swollen whereas the hydrophobic PS nanophases remain unaffected while the PNIPAAm-*g*-PS networks were subjected to the swelling experiments; the PS nanodomains could act as the additional physical crosslinking points of PNIPAAm chains. This judgment can be further confirmed by examining the self-assembly behavior of the model PNIPAAm-*b*-PS diblock copolymers in water. Owing to the high hydrophobicity of PS and water-solubility of PNIPAAm, it is expected that the amphiphilic diblock copolymers would be self-organized into the structures of micelles in water. The size of the micelle is readily measured by means of photon correlation spectroscopy (PCS). Shown in Fig. 8 are the plots of size of the micelle particles in the aqueous PNIPAAm copolymers containing 5 and 20 wt% PS. It is seen that in the aqueous copolymers, the sizes of the micelle particles are about 290 and 450 nm, possessing the quite narrow distribution of size. It should be pointed out that the sizes of PS domains detected by means of PCS is not necessarily identical with those by means of AFM since there is the methodological difference between AFM and PCS techniques. The former reflects the information about tip–specimens interactions resulting from adhesion, surface stiffness and viscoelastic

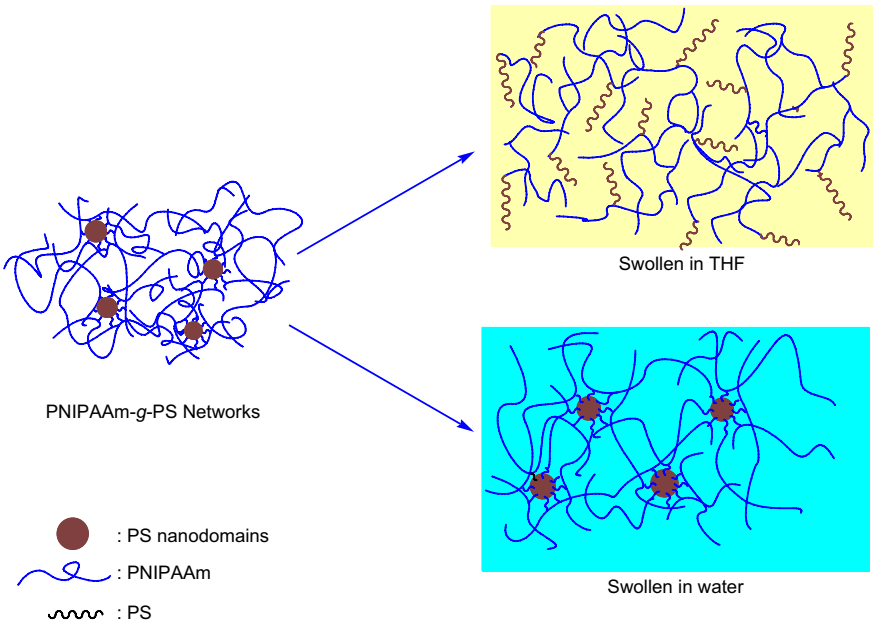

Scheme 2. Swelling behavior of PNIPAAm-*g*-PS networks with THF and water.

effects in bulk [64–69]. The PCS measurement is on the basis of the fluctuations of concentration and density of aqueous samples, which cause the local dielectric constant to change and thus in turn gives rise to fluctuations in frequency and intensity of the scattered light. It is plausible to propose that the size of micelle detected with PCS could span from the centers of the PS nanodomains to the region around the nanodomains. Therefore, the AFM results could be more sensitive to the sizes of PS nanodomains. In views of the results of PCS, it is proposed that the PS nanodomains existed in the swollen PNIPAAm-*g*-PS hydrogels.

The presence of PS nanodomains could exert a profound impact on the swelling, deswelling and reswelling behavior of the hydrogels. While the PNIPAAm-*g*-PS crosslinked copolymers were subjected to the swelling experiments, the hydrophilic component (*viz.* PNIPAAm chains) will form the stable hydration interactions with aqueous medium *via* hydrogen bonding interactions between the amide moiety (–CONH–) and water molecules at the temperature below the LCST. In addition to the hydrophilic part, there are a great number of hydrophobic PS nanodomains in the hydrogels. The hydrophobic microdomains could behave as the microporogens and thus the area of the contact interfaces between PNIPAAm chain and water molecules is significantly increased. The increased contact interfaces will facilitate the diffusion of water molecules in the crosslinked networks and thus the rates of swelling, deswelling and reswelling were increased (See Figs. 4–6). Owing to the hydrophobic component (*viz.* PS), the volume-phase transition temperatures of the hydrogels shifted to the lower temperatures (Fig. 4). In the PNIPAAm hydrogels the aggregated PS microdomains could additionally act as the physical crosslinking sites of the hydrogels and the thus the overall crosslinking density of the hydrogels was increased (See Figs. 4–6). The higher the PS contents in the hydrogels the higher the crosslinking density. Therefore, the dependence of hydrogel behavior on crosslinking density should be displayed for the PNIPAAm-*g*-PS hydrogels. The experimental results indeed showed that the swelling (and/or deswelling and reswelling) behavior is indeed quite dependent on the content of PS in the PNIPAAm-*g*-PS hydrogels. In addition, it is noted that the mechanical strength of the materials was improved due to the presence of the physical crosslinking sites (*i.e.*, PS nanodomains). It is of interest to note that the PNIPAAm-*g*-PS hydrogels are capable of sustaining the experiments of several cycles of swelling, deswelling and reswelling experiments and the shapes of all the specimens of hydrogels were well reserved and no significant depression in mechanical strength was exhibited. This case is in marked contrast to the conventional PNIPAAm hydrogels, which could be important for the application of hydrogels.

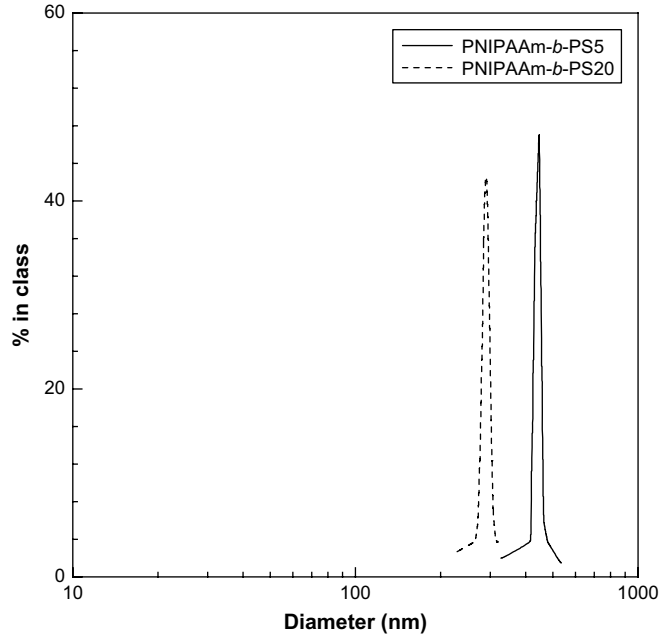

Fig. 8. Plots of size of the micelle particles for the aqueous solutions of PNIPAAm-*b*-PS diblock copolymers.

4. Conclusion

Reversible addition–fragmentation chain transfer polymerization was used to prepare the crosslinked poly(*N*-isopropylacrylamide)-*graft*-polystyrene copolymer networks (PNIPAAm-*g*-PS). Due to the immiscibility of PNIPAAm with PS, the PNIPAAm-*g*-PS crosslinked copolymers displayed the microphase-separated morphology. Using

the linear model PNIPAAm-*b*-PS diblock copolymers, the nanostructures were further investigated by means of atomic force microscopy (AFM). While the PNIPAAm-*g*-PS copolymer networks were subjected to the swelling experiments, it is found that the PS block-containing PNIPAAm hydrogels significantly exhibited faster response to the external temperature changes according to swelling, deswelling, reswelling experiments than the conventional PNIPAAm hydrogels. The improved thermo-responsive properties of hydrogels have been interpreted on the basis of the formation of the specific microphase-separated morphology in the hydrogels, *i.e.*, the PS chains pendent from the crosslinked PNIPAAm networks were self-assembled into the highly hydrophobic nanodomains, which behave as the microporogens and thus promote the contact of PNIPAAm chains and water. The self-organized morphology was further confirmed by photon correlation spectroscopy (PCS). The PCS shows that the linear model block copolymers of PNIPAAm-*g*-PS networks were self-organized into micelle structures and the PS domains constitute the hydrophobic nanodomains in PNIPAAm-*g*-PS networks.

Acknowledgements

The financial supports from Natural Science Foundation of China (No. 20474038 and 50873059) and National Basic Research Program of China (No. 2009CB930400) are acknowledged. The authors thank Shanghai Leading Academic Discipline Project (Project Number: B202) for the partial support.

References

[1] Wichterler O, Lim D. Nature 1960;185:117.
[2] Drossi D, Kajiwara K, Osada Y, Yamauchi A, editors. Polymer gels. New York: Plenum; 1991.
[3] Okano T, editor. Biorelated polymer and gels. Boston: Academic; 1998.
[4] Hoare TR, Kohane DS. Polymer 1993;2008:49.
[5] Hirokawa Y, Tanaka Y. J Chem Phys 1984;81:6379.
[6] Matuo ES, Tanaka T. J Chem Phys 1988;89:1695.
[7] Suzuki A, Tanaka T. Nature 1990;346:345.
[8] Ding YW, Ye XD, Zhang GZ. Macromolecules 2005;38:904.
[9] Otake K, Inomata H, Konno M, Saito S. Macromolecules 1990;23:283.
[10] Inomata H, Goto S, Ohtake K, Saito S. Langmuir 1992;8:687.
[11] Shibayama M, Morimoto M, Nomura S. Macromolecules 1994;27:5060.
[12] Wu C, Zhou SQ. Phys Rev Lett 1996;77:3053.
[13] Liang L, Rieke PC, Liu J, Fryxell GE, Young JS, Engelhard MH, et al. Langmuir 2000;16:8016.
[14] Yin X, Hoffman AS, Stayton PS. Biomacromolecules 2006;6:1382.
[15] Heskins M, Guillet JE, James E. J Macromol Sci Chem 1968;A2:1441.
[16] Kujawa P, Tanaka F, Winnik FM. Macromolecules 2006;39:3048.
[17] Schild HG. Prog Polym Sci 1992;17:163.
[18] Wu C, Zhou S. Macromolecules 1997;30:574.
[19] Wu C, Zhou S. Polymer 1998;39:4609.
[20] Kujawa P, Winnik FM. Macromolecules 2001;34:4130.
[21] Zhang W, Shi L, Ma R, An Y, Xu Y, Wu K. Macromolecules 2005;38:8850.
[22] Xu Y, Shi L, Ma R, Zhang W, An Y, Zhu XX. Polymer 2007;48:1711.
[23] Crowther HM, Vincent B. Colloid Polym Sci 1998;276:46.
[24] Zhu PW, Napper DH. J Colloid Interface Sci 1996;177:343.
[25] Zhu PH, Napper DH. Chem Phys Lett 1996;256:51.
[26] Zhu PH, Napper DH. Macromol Chem Phys 1999;200:1950.
[27] Mamada A, Tanaka T, Kungwatchakun D, Irie M. Macromolecules 1990;23:1517.
[28] Kato E. J Chem Phys 1997;106:3792.
[29] Takigawa T, Araki H, Takahashi K, Masusa T. J Chem Phys 2000;113:7640.
[30] Kato N, Tkahashi F. Bull Chem Soc Jpn 1997;70:1280.
[31] Xulu PM, Filipcsei G, Zrinyl M. Macromolecules 2000;33:1716.
[32] Haraguchi K, Farnworth R, Ohbayashi A, Takehisa T. Macromolecules 2003;36:5732.
[33] Nakamoto C, Motonaga T, Shibayama M. Macromolecules 2001;34:911.
[34] Yoshida R, Uchida K, Kaneko Y, Sakai K, Kikuchi A, Sakurai Y, et al. Nature 1995;374:240.
[35] Haraguchi K, Takehisa T. Adv Mater 2002;14:1120.
[36] Wu X, Hoffman AS, Yagger P. J Polym Sci Part A Polym Chem 1992;30:2121.
[37] Zhuo R-X, Li W. J Polym Sci Part A Polym Chem 2003;41:152.
[38] Norihiro K, Yasuzo S, Shihoko S. Macromolecules 2003;36:961.
[39] Zhang X-Z, Yang Y-Y, Chung T-S, Ma K-X. Langumuir 2001;17:6094.
[40] Serizawa T, Wakita K, Akasika M. Macromolecules 2002;35:10.
[41] Zhang J, Chu L-Y, Li Y-K, Lee YM. Polymer 2007;48:1718.
[42] Dinu MV, Ozmen MM, Dragan ES, Okay O. Polymer 2007;48:195.
[43] Unal B, Hedden RC. Polymer 2006;47:8173.
[44] Zhang X-Z, Yang Y-Y, Chung T-S. Langmuir 2002;18:2538.
[45] Ma X, Cui Y, Zhao X, Zheng S, Tang X. J Colloid Interface Sci 2004;276:53.
[46] da Silva R, de Oliveira MG. Polymer 2007;48:4114.
[47] Ju HK, Kim SY, Lee YM. Polymer 2000;42:6851.
[48] Kobato N, Matsubara T, Eguchi Y. J Appl Polym Sci 1998;70:1027.
[49] Annaka M, Matsuura T, Kasai M, Nakahira T, Hara Y, Okano T. Biomacromolecules 2003;4:395.
[50] Kayaman N, Kazan D, Erarslan A, Okay O, Baysal BM. J Appl Polym Sci 1998;67:805.
[51] Guiseppi-Elie A, Sheppard NF, Brahim S, Narinesingh D. Biotechnol Bioeng 2001;75:475.
[52] Zhang W, Shi L, Wu K, An Y. Macromolecules 2005;38:5743.
[53] Zhang X-Z, Zhuo R-X. Langmuir 2001;17:12.
[54] Haraguchi K, Takehisa T, Fan S. Macromolecules 2002;35:10162.
[55] Farnworth R, Ohbayashi A, Takehisa T. Macromolecules 2003;36:5732.
[56] Mu J, Zheng S. J Colloid Interface Sci 2007;307:377.
[57] Can V, Abdurrahmanoglu S, Okay Q. Polymer 2007;48:5015.
[58] Gomez ML, Fasce DP, Williams RJJ, Erra-Balsells R, Fatema MK, Nonami H. Polymer 2008;49:3648.
[59] Iyer G, Viranga Tillekeratne LM, Coleman MR, Nadarajah A. Polymer 2008;49:3744.
[60] Liu F, Tao GL, Zhuo RX. Polym J 1993;25:561.
[61] Le TP, Moad G, Rizzardo E, Thang SH. PCT Int Appl WO 9801478 A1 9801115.
[62] Olabisi O, Robeson LM, Show MT. Polymer–polymer miscibility. New York: Academic Press; 1979.
[63] Utracki LA. Polymer blends and alloys. New York: Hanser Publisher; 1989.
[64] Jayalakshmi R, Ramadas SR, Pillai CN. Org Prep Proced Int 1981;13:71.
[65] Schmitz I, Schreiner M, Friedbacher G, Grasserbauer M. Appl Surf Sci 1997;115:190.
[66] Magonov SN, Elings V, Whangbo MH. Surf Sci 1997;375:L385.
[67] Tamayo A, Garcia R. Langmuir 1996;12:4434.
[68] Chen X, McGurk SL, Davies MC, Roberts CJ, Shakesheff KM, Tendler SJB, et al. Macromolecules 1998;31:2278.
[69] Clarke S, Davies MC, Roberts CJ, Tendler SJB, Williams PM, Lewis AL, et al. Macromolecules 2001;34:4166.